4. Beamlines

This section describes the activity status of the beamlines in FY2022. It includes frontend, optics and transport channel of SPring-8, and SACLA beamlines. In addition to routine maintenance, several component upgrades and R&D were performed. Beamline upgrade and portfolio rearrangement are ongoing toward the SPring-8 major upgrade. Some beamline reconstructions were carried out during this period.

1. Frontend

1-1. High-heat-load handling techniques

Based on the study of inclusion dispersion in GlidCop, an attempt was made to use fracture mechanics methods to predict the crack propagation life of a test piece subjected to a fatigue fracture in a cyclic heat loading test using an electron beam irradiation system. The initial crack shape was assumed to be three types of semi-ellipse with a fixed height (b) of 100 μm and total widths (2a) of 10, 30, and 100 μm, namely, b/a=20, 6.67, and 2. In addition, crack growth was inferred to propagate independently based on the respective stress intensity factors in the width and depth directions. According to the calculated crack growth rate using the Paris law approximation at 200°C, the larger the b/a (i.e., elongated crack shape), the slower the crack growth. Overall, the predicted results are longer than the actual fracture life. It was also found that in cases where b/a is large, crack propagation in the width direction tends to precede and eventually converges to a shape where b/a is approximately 1.

1-2. X-ray beam position monitor (XBPM)

Evaluation tests of the pulse mode X-ray beam position monitor (PM-XBPM), which was developed using SPring-8's original technology, were conducted at the insertion device beamline. The resolution was systematically evaluated by changing the bunch current of the storage ring, and it was confirmed that the resolutions of 4.5 μm std (horizontal)/4.5 μm std (vertical) were obtained for the electron bunch with a beam current of 5 mA/bunch. It was also confirmed that the resolutions of 1.7 μm std (horizontal)/1.2 μm std (vertical) can be obtained by appropriately using a low-pass filter. We attempted to observe the pulse-by-pulse behavior of the synchrotron radiation beam during user operation using the PM-XBPM. Observations were made for all pulses in the "203 bunches mode" and for an isolated pulse in the "11/29-bunches + 1 bunch mode". For the first time in the world, we succeeded in quantitatively observing oscillation phenomena for each pulse immediately after the injection into the storage ring.

1-3. Energy-resolved beam monitoring system (ES-XBPM) for X-ray beam exiting from the frontend

To promote the practical application of ES-XBPM, which has been fundamentally developed at BL05XU, R&D was started by installing a new vacuum chamber with a test stand at BL03XU. The mechanical stopper and limit switch were repositioned so that the diamond thin film could be moved in and out of the photon beam axis regardless of whether the MBS was opened or closed. Furthermore, an experiment was conducted using CITIUS, a two-dimensional detector with high frame rate and high energy resolution that is being developed by RIKEN, so that a clear energy-resolved beam image could be successfully

acquired. This confirmed that this method is excellent for observing the spectrum, spatial distribution by wavelength, and beam axis of the undulator radiation all at once. In addition, we started to study Timepix/Medipix [1] as a candidate for other detectors, and scanning measurements using SDD were also examined.

2. Optics and Transport Channel

2-1. Commissioning of BL13XU optics

At the end period of FY2021, BL13XU was upgraded to effectively integrate a crystal diffraction apparatus. At the same time, we improved the double-crystal monochromator (DCM) and the horizontal mirror. In the DCM, two pairs of silicon crystals were installed with 111 and 311 reflection net planes, which are selectable by moving horizontal translation stages. The energy range was extended to 72.33 keV with 311 reflection from the previous maximum of 37.77 keV with 111 reflection. The height of the first crystals was increased from 35 mm to 70 mm in order to increase thermal contact between the crystals and liquid-nitrogen-cooled copper clamps. The update of the control program shortened the operation time needed for energy change. The time was reduced to 4 min to move the Bragg angle from 3 deg (energy 37.77 keV for 111 reflection) to 27 deg (4.35 keV). On the other hand, the horizontal mirror to cut the higher order harmonics was replaced by a mirror polished by a novel polishing technique to obtain a highly flat surface. In the first quarter of FY2022, the optics were adjusted successfully. Figure 1 shows the beam images behind the mirror before and after the improvement.

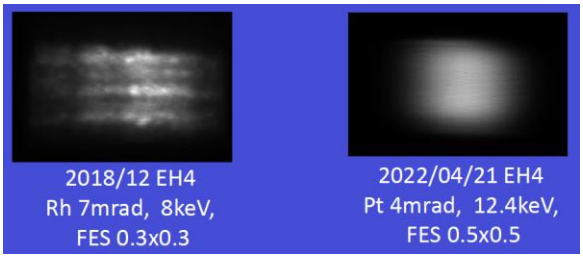

Fig. 1. Beam images behind the horizontal mirror before (left) and after the improvement (right).

2-2. Installation of ultrahigh-vacuum DCM to BL20B2

BL20B2 is the only bending-magnet beamline with a total length of 215 m. The DCM covers the energy ranges of 4.35–37.77 keV with silicon 111 reflection and 8.34–72.33 keV with 333 reflection. Before FY2021, the net planes had been changed by replacing the crystals by hand.

During the downtime between FY2021 and FY2022, the new DCM was installed. The DCM has long horizontal translation stages to change the net planes of the horizontally arranged crystals. In addition, the mechanism was designed to adapt to the ultrahigh-vacuum condition. This is because the beamline was equipped with the two sets of double-multilayer monochromators, and therefore, pollution and contamination must be reduced.

2-3. Upgrade of optics hutch of BL46XU

BL46XU was reconstructed for exclusive use for HAXPES applications from December 2022. Figure 2 shows a schematic view of the optical arrangement in the optics hutch. To reduce speckle and fringe patterns of X-ray beams, the frontend beryllium windows were removed and a newly designed differential pump chamber was installed. The DCM with silicon 111 reflection was improved to increase thermal contact between the crystals and

liquid-nitrogen-cooled copper clamps. As new optical components, the beamline was equipped with two double channel-cut monochromators (DCCMs), an X-ray phase retarder (XPR), and a beam intensity/position monitor. The DCCMs are used in the (+, -, -, +) reflection arrangement of 220 or 311 reflection, in accordance with wanted energy bandwidths. Commissioning will start in April 2023.

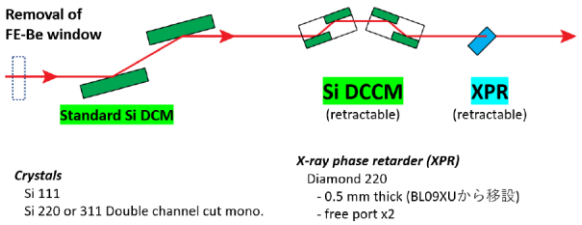

Fig. 2. Schematic view of the optical arrangement in the optics hutch.

2-4. Wide field of view imaging with high-flux 100-keV X-rays using a reflective beam expander

In BL05XU, high-flux 100-keV X-rays are available for the high-speed imaging of metallic bulky samples. However, the vertical direction of the field of view is narrow owing to the beam size of incident X-rays. To expand the vertical beam size, we designed, installed, and evaluated a reflective beam expander consisting of a W/C laterally graded multilayer on a hyperbolic convex mirror. By employing a multilayer, the grazing angle and aperture can be enlarged and high reflectivity can be achieved, even for 100-keV X-rays. The multilayer was deposited at a SPring-8 in-house laboratory. Figure 3 shows a photograph of the reflective beam expander. As a result of the evaluation at BL05XU, high-flux 100-keV X-rays with a wide field of view of 5 mm square are available.

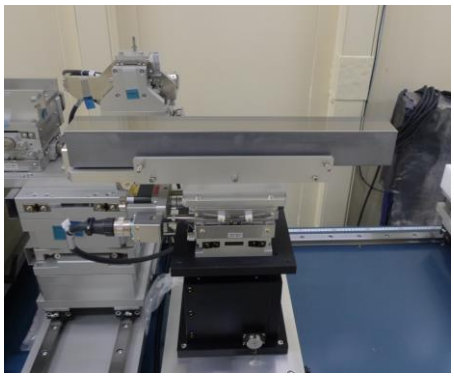

Fig. 3. Photograph of reflective beam expander for 100-keV X-rays.

2-5. Upgrade of focusing mirrors in BL46XU

In conjunction with the upgrade of BL46XU, the installation of monolithic Wolter type-I focusing mirrors was carried out in the experimental hutch (EH) 1 and EH2. The mirror in EH1 has the same optical design as used in BL09XU EH1, with a magnification of 1/27. On the other hand, the mirror in EH2 was newly designed to meet the requirements with a smaller magnification of 1/50. The commissioning and evaluation will be carried out in 2023A.

2-6. Design of optical systems for the upgrade of BL39XU

The upgrade of BL39XU is planned for FY2023. Optical systems, such as the K–B focusing mirror for EH1, the monolithic Wolter focusing mirror for the new EH2, and the coaxial-output higher-order-suppression mirror system, were designed and will be installed by the end of 2023.

2-7. Design of optical components in optics hutch of BL15XU

At BL15XU, we have designed the optical components in the optics hutch (OH) for X-ray analyses with the 100-keV high-flux beam, such as 3-dimensional X-ray diffraction (3D-XRD) and the pair distribution function (PDF). After the

modifications, this beamline is scheduled to start optical components commissioning with the X-ray beam in 2024. The double-multilayer monochromator (DMM) can extract a 1% energy bandwidth (B.W.) beam from the undulator higher-order radiation and form a high-flux beam about 300 times higher than that of a conventional SPring-8 standard silicon double-crystal monochromator (DCM).

At BL15XU, a 100-keV 1% B.W. beam can be exclusively supplied to experimental hutches without the DCM. The optical instrument arrangement is shown in Fig. 4. The DCM consists of mirrors with 150 Cr/C pairs and can provide a horizontal beam by two reflections of M1 and M2, as shown in Fig. 4. The total reflection low-energy component reflected by the DMM is removed by attenuators (ATTs) placed upstream. Indirect water-cooled diamond, SiC, Si, and Mo are used for the ATT materials in multiple steps. For the 100-keV DMM beam use, the equipment is designed in the OH to take shielding into account and to handle the 400-W-class heat load that leaves the frontend (FE) slit. Other major components such as water-cooled beam catchers (BCs), beam profile monitors (BMs), four-blade slits (transport channel (TC) slits), etc., were fabricated to handle the heat load.

3. Beamlines of SACLA

3-1. XFEL beamlines

The two XFEL beamlines (BL2 and BL3) were stably operated in parallel throughout FY2022 and produced hard X-ray pulses in the energy range of 4–20 keV [2]. The main linac of SACLA, which is typically operated at the 60 Hz repetition rate, drives both beamlines by switching the electron-beam route on a pulse-by-pulse basis. Furthermore, SACLA injects electron beams into SPring-8 for its stable operation.

In this fiscal year, a new in-line spectrometer with an improved resolution was installed for the X-ray transport channels to monitor the spectra of each XFEL pulse. The new in-line spectrometer was designed to utilize a capillary filled with diamond microcrystals for this purpose. The previous in-line spectrometer consisting of a nanocrystalline-diamond foil could provide accurate information on peak photon energies [3]. However, its energy resolution was not sufficient to capture detailed spectral shapes. Enhancements in the spectral resolution of the spectrometer have been pursued to enable the control of the spectral properties using an automated tuning system based on machine learning technologies. Note that machine tuning had been previously applied to optimize the accelerator parameters mainly for maximizing the pulse energy. The ability to control the spectral properties was the next target to establish the unique capability of producing optimized XFELs for each user experiment.

Following the successful test experiment with a prototype of the spectrometer [4] in FY2021, new spectrometers (Fig. 5) were built and installed in the transport channels at BL2 and BL3 during FY2022. These updated spectrometers are operational either with the conventional nanodiamond foil or the capillaries filled with microcrystals. The capillary is used for precise accelerator fine-tuning with the spectral resolution of several eV before each user experiment. Conversely, the nanodiamond foil is suitable for continuous monitoring during experiments. These new spectrometers are now routinely used for accelerator tunings and user operations.

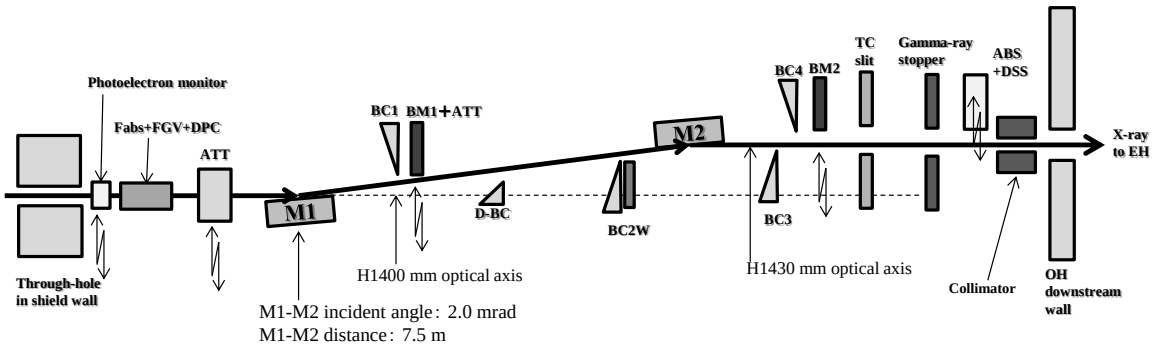

Fig. 4. Optical layout of beamline components in optics hutch (OH) of BL15XU. Fabs: fast absorber, FGV: fast gate valve, DPC: differential pump chamber, ATT: attenuator, M (M1, M2): mirror, BC: beam catcher, D-BC: direct BC, BC2W: BC with tungsten, BM: beam profile monitor, TC: transport channel, ABS: absorber, DSS: downstream shutter.

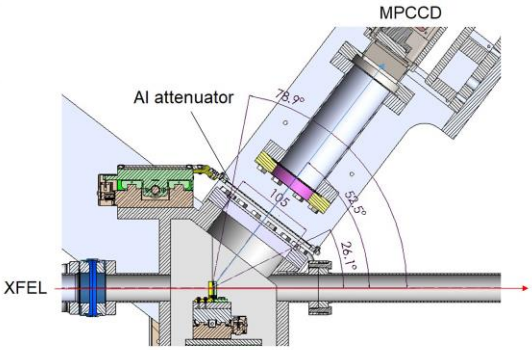

Fig. 5. Schematic drawing of the new in-line spectrometer. Diffracted X-rays from the nanodiamond foil or capillaries in the vacuum chamber are captured with an MPCCD detector.

degradation of the undulator magnets after the replacement of the undulator units in March 2021 following the considerable reduction in output pulse energy.

The full autotuning software for beamline instruments has been implemented at BL1 after the successful utilization of a similar system at the hard X-ray beamlines of BL2 and BL3. The beamline tunings had been conducted manually before every user beamtime by two to three facility staff members. The autotuning system can finely adjust the photon energy of the SXFEL and the optical axis after the offset mirror with a higher reproducibility within a shorter tuning time.

3-2. Soft X-ray FEL beamline

The soft X-ray (SX) FEL beamline (BL1), which is driven by a dedicated 800 MeV linac (SCSS+), was stably operated with the photon energies of 40–150 eV and the averaged pulse durations of ~30 fs [5, 6]. In FY2022, the output FEL energy was kept almost at the same level of ~50 μJ at 100 eV. The constant energy output implies that there was no significant

Takahashi Sunao[*1], Ohashi Haruhiko[*2], Yamazaki Hiroshi[*2], Senba Yasunori[*2], Yumoto Hirokatsu[*2], Koyama Takahisa[*2], Inubushi Yuichi[*3], Owada Shigeki[*3], Ichiro Inoue[*4], Yabuuchi Toshinori[*3], Tono Kensuke[*3], and Yabashi Makina[*4]

[*1]Innovative Synchrotron Radiation Facility Division, RIKEN SPring-8 Center

[*2]Beamline Division, JASRI

[*3]XFEL Utilization Division, JASRI
[*4]XFEL Research and Development Division, RIKEN SPring-8 Center

References

[1] https://www.raddvc.co.jp/product/detector/425.html.
[2] Tono, K. et al. (2019). *J. Synchrotron Rad.* **26**, 595–602.
[3] Tono, K. et al. (2013). New J. Phys. 15, 083035.
[4] Inoue, I. et al. (2022). J. Synchrotron Rad. 29, 862–865.
[5] Owada, S. et al. (2018). J. Synchrotron Rad. 25, 282–288.
[6] Owada, S. et al. (2020). J. Synchrotron Rad. 27, 1362–1365.